Contents lists available at GrowingScience

Current Chemistry Letters

homepage: www.GrowingScience.com

Mesoporous MCM-41 modified with Cu(II) for indole removal: A Taguchi design

S. A. Khoshkarvandani[a], R. Fazaeli[a*], M. G. Saravani[a] and H. Pasdar[b]

[a]*Department of Chemistry, South Tehran Branch, Islamic Azad University, Tehran, Iran*
[b]*Department of Chemistry, North Tehran Branch, Islamic Azad University, Tehran, Iran*

C H R O N I C L E

Article history:
Received October 11, 2019
Received in revised form
April 9, 2020
Accepted April 9, 2020
Available online
April 14, 2020

Keywords:
Cu(II)/MCM-41
Mesopore
Indole
Taguchi
Optimization

A B S T R A C T

Indole is a hazardous substance existing in the curl oil, which released to the environment by various industrial activities; thus, decreasing its ratio from nature seems to be essential. In this study, a facial pathway for loading Cu(II) particles on MCM-41 mesoporous material was introduced as an efficient catalyst for indole oxidation. The obtained catalyst was characterized by XRD, FESEM, EDS, TEM and BET/BJH techniques. Based on Taguchi method, indole oxidation via prepared catalyst at mild condition was evaluated. By applying this method, the operating factors including Indole initial concentration (mg/L), pH value and the mass of catalyst (g) were optimized. It was found that pH plays the most crucial role in indole oxidation, on the other word, in alkaline environment; indole oxidation was happened with higher yield.

1. Introduction

Nowadays, due to human activities, air and water pollutions considered as a global issue.[1] Scientists are challenging vigorously to reduce the amounts of contaminant. One of the most crucial sources of air pollution is the oxidation of the nitrogen-containing compounds, which are existence in the crude oil such as carbazols, pyridines and indoles.[2] Such substances are combined with oxygen while burning, producing NO, and a colorless and toxic gas. As it released into the air, it reacts with the available oxygen in the atmosphere and generates NO_2. Moreover, NO_2 gases plays a critical role in the acidic rain, as they tend to decompose into the nitric acid, they release one oxygen from each molecules and produce O_3 (ozone). Actually, NO_2 is responsible for brown color in smoggy air, an important factor in creating photochemical smog, and O_3 is a toxic substance that causes eye irritation.[3] Besides, the nitrogen-containing compounds are a serious obstacle in the refining petroleum, since themselves or their products settled on the acidic sites of catalysts and make these sites inaccessible to the sulfur-containing compounds.[4] Inole is an aromatic and toxic compound that is introduced to the environment by development of industry in various realms such as fuel industry, pesticides, and cosmetics.[5-7] Since indole and its derivations are entered into the ecosystem in a variety of ways, like oxidation of fossil fuels and factories effluents, they considered as an air and water pollutant. So far, many efforts have been made to control the amount of indole released into the environment, like chemical and biological

* Corresponding author.
E-mail address: r.fazaeli@iran.ir (R. Fazeli)

doi: 10.5267/j.ccl.2020.4.002

cleansing that unfortunately led to formation of the other toxic and carcinogen compounds. Other denitrognation methods that were widely used in the petroleum industry required harsh and expensive operation conditions such as high temperature and pressure and catalyst loss.[8,9] Bearing the aforementioned points in mind, there is still a need for designing a low cost, reusable, environmentally friendly catalyst with high adsorption capacity. Efforts to solve this problem have led to introduction of many porous materials. These materials, due to their large volume of cavities, not only have a high contact surface, like homogeneous catalysts, but are capable of separation and used for several times, as homogeneous catalysts.[10] Cavity size is a crucial factor in the ratio of their selectivity and their classification, according to this issue, if their pore size are smaller than 2 nm they were called as microporous, between 2 to 50 nm as mesoporous and larger that 50 nm, as macroporous.[11] One of the most popular type of porous materials is zeolites, their main advantages are, being ease of installation, low energy consumption and usability under mild conditions.[12] Although, the size of pores makes zeolites extremely selective, but they are not an appropriate adsorbant for relatively larger molecules. In the comparison with zeolites, Mobile Composition of Mater (MCM) materials, due to their large and uniform cavities and high surface area are very suitable candidantes for the larger moleculs.[13] Owing such incredible properties also made them a proper bed for immobilization of metal ions and metal oxides. In fact, it is an effective approach for increasing the catalytic activity of such materials by loading these substances on the mesoporous materials. Nikoorazm synthesized the Ni(II)-Vanillin complex and immobilized it on MCM-41 nanostructure for introducing a green, reusable, economic and effective catalyst for multicomponent reactions, which was easy to remove from the reaction mixture and reusable for several times.[14] Wei and Wang, successfully synthesized MCM-41@mTiO_2 by combining sol-gel and hydrothermal methods. The obtained composite was employed for dinitro butyl phenol degradation. The results indicate that loading TiO_2 on the MCM-41 increased its photocatalyst activity, which makes it an efficient catalyst for degradation hazardous contaminants from the wastewater.[15] Recently, statistical and mathematical techniques such as Design of Experiments (DOE), provides a great opportunity for optimizing the experiment conditions. Among all of them, there are several preference of Taguchi method such as requiring fewer runs, considering the reaction between factors, requiring less time and cost.[16]

2. The experiments

2.1. Materials

Sodium hydroxide, hydrochloric acid, copper (II) chloride, Cetyltrimethylammounium bromide (CTAB), tetraethyl orthosilicate (TEOS), and Indole were purchased from Merck Germany. All the chemicals were employed without any further purification.

2.2. Preparation of MCM-41

In order to synthesis MCM-41, at first, a solution containing 1 L distilled water, 2 g CTAB and NaOH 2M were shaken for 30 min at 353 K. In the second step, TEOS was added drop by drop to the fine white particles are revealed. In the third step, the suspension refluxed for 120 min at the same temperature. In the next step, the obtained mixture cooled down and then, filtered and washed for several times. The resulting material rested at room temperature overnight. In the last step, it was placed in a furnace with the heating ratio of 2°/min to the point that it reached 823 K, and then remained in that temperature for the other 60 min.[17]

2.3. Preparation of Cu(II)/MCM-41

To prepare the Cu(II)/MCM-41 composite, 5g of synthetic MCM-41 was dispersed in a solution containing of 100 mL Cu^{2+} 0.2 M, the resulted suspension was stirred for 24h. After that, it centrifuged for three times and then, placed in an oven for 180 min at 283 K. Finally, the product was calcinated at 723 K for 12h.

2.4. Design of Experiments Based on The Taguchi technique

This useful method was introduced by Genichi Taguchi in 1960.[18,19] Using this method provides a great opportunity to obtain the optimum experimental circumstances with the lowest number of experiences, which not only save time, but decrease the costs. In this way, by regarding the amounts of factors and levels, various orthogonal arrays as matrix experiments are use. By applying Taguchi methods variability can be shown by signal to noise rate. The highest amount of S/N rate shown the optimal condition. The orthogonal arrays are presented by the following formula: $L_n (X^y)$ where n the amount of designed experiments, which X is the number of levels and y is the maximum amount of factors, investigating by array.[20] In this work, three effective factors including H_2O_2, indole initial concentration (IND concentration), and PH, each in 3 levels are considered. Table 1 presents the investigated factors with their related levels. After introducing the studied factors and their related levels, the 9 experiments were suggested by the software, which are shown in Table 2.

Table. 1. Factors and their related levels employed in DOE.

Number of levels	pH	IND concentration	Mass of Catalyst
1	**4**	**8**	**0.1**
2	**7**	**16**	**0.5**
3	**10**	**32**	**1.0**

Table. 2. Responses, S/N ratio and means

Experiment no.	pH	IND Concentration (ppm)	Mass of Catalyst	Removal (%)	S/N ratio
1	4	8	0.1	76	32.6694
2	4	16	0.5	79	32.0412
3	4	32	1.0	90	35.5630
4	7	8	0.5	81	36.6502
5	7	16	1.0	85	38.5884
6	7	32	0.1	79	34.3201
7	10	8	1.0	89	37.3846
8	10	16	0.1	98	34.3201
9	10	32	0.5	91	33.0648

2.5. Reaction Procedure

1g of prepared catalyst was added to 20 ml indole solution with different initial indole concentration, then, the H_2O_2 was added to the solution. The obtained suspension shaken under UV- C16W lamp radiation. After 40 minutes it was centrifuged at 10000 rpm for 10 minutes due to separating the catalyst from solution. For measuring the ratio of indole removal, UV-vis spectrophotometer (pg instruments, T80+) was used. In order to calculation of efficiency of indole removal via the prepared composite the following equation was used:

$$\text{Efficiency (\%)} = \frac{(A_0 - A_f)}{A_0} \times 100$$

where A_0 and A_f are the initial and final concentration of indole, respectively.

3. Results and Discussion

3.1. XRD analysis

In order to evaluate the crystallinity and the structure of the synthesized catalysts, X-ray diffraction analysis was used (Rigaku, Ultima IV). **Fig. (1a)** illustrated the low angel XRD trend of the synthesized MCM-41. The characteristic peaks of MCM-41, at 2θ= 2.51°, 4.31° and 4.79°, corresponding to (100), (110) and (200) Miller indices, respectively, which are commonly used for identify MCM-41from this region (00-038-0241). The appearance of such peaks indicates that MCM-41 is synthesized with hexagonal structure. Figure (1b) shows the XRD patterns of MCM-41 and Cu(II)/MCM-41. Although

after loading Cu(II) particles on the MCM-41, it's over structure did not changed, the intensity of its characteristic peaks decreased and shifted to higher 2θ. These observants indicate that Cu(II) particles are trapped inside the MCM-41 channels, causing their structure to become amorphous.[21] Moreover, for obtaining the crystal size of the catalyst Debye-Sherer equation was employed:

$$D = \frac{k\lambda}{\beta cos\theta},$$

where D is the crystalline dimension, k is a constant, λ is the wave length of the cathode and β is referring to FWHM. By applying this method, the crystal size of MCM-41 was obtained between 8 to 17nm, and the average particles crystal size was estimated to be 9.5nm[22] (**Fig. 1**).

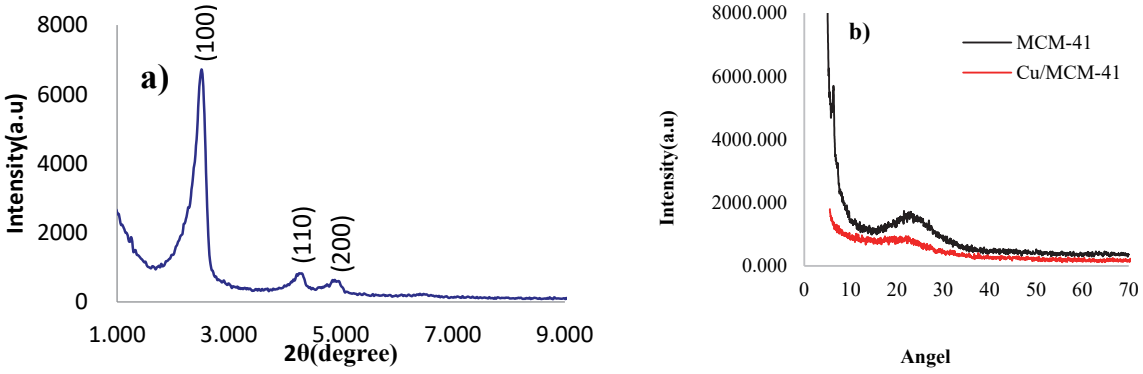

Fig. 1. X-ray diffraction analysis.

3.2. FESEM Analysis

The morphology of the synthesized catalyst was investigated by applying Field Emission Scanning Electron Microscopy (FEI NOVANANOSEM 450 ELECTRON MICROSCOPE). **Fig. 2 (a, b)** shows the FESM images of MCM-41 and Cu(II)/MCM-41 composite, respectively. The obtained data confirm that the synthesized MCM-41 has a uniform and spherical morphology. The mean diagram of MCM-41 seems to be 864.1 nm. However, after loading Cu(II) particles MCM-41 virtually conserve its initial morphology, while Cu(II) particles properly dispersed on its surface.

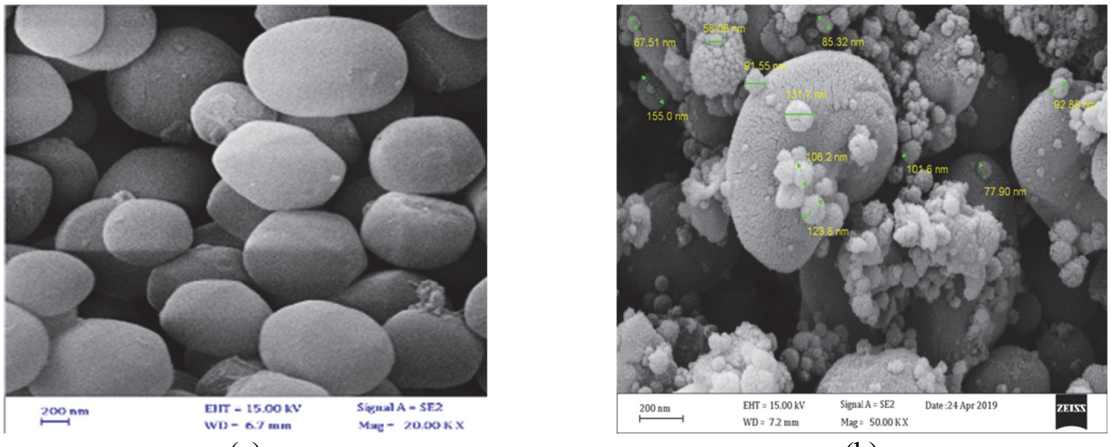

(a) (b)

Fig. 2. FESEM images of a) MCM-41 and b) Cu(II)/MCM-41

3.3. EDS Analysis

For evaluating the consist chemical elements and their weight percentage (wt. %) the X-ray dispersive (Bruker, X Flash6l10) was employed. It is observed that the containing elements are include Si (54.1 %), O (41.8%), Al (0.2%), Cu (3.4%) (**Fig. 3**).

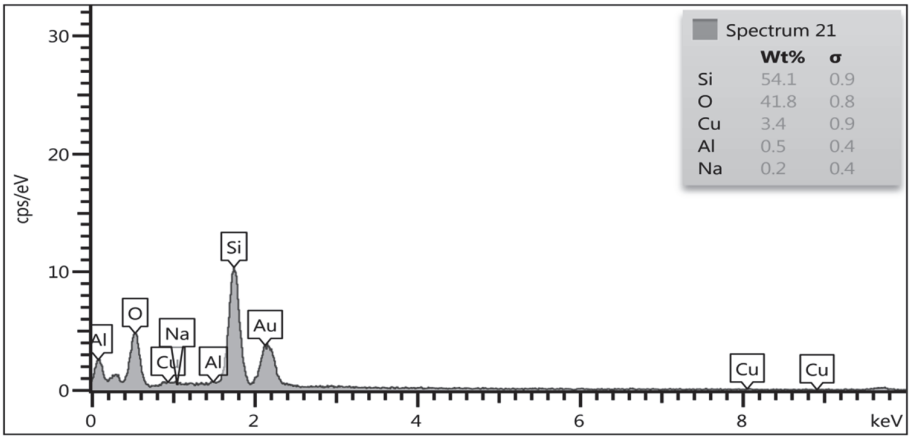

Fig. 3. EDX of the Cu(II)/MCM-41.

3.4. TEM Analysis

Transmission electron microscopy (TEM) image of the Cu(II)/MCM-41 is shown in **Fig. 4**. The ellipse shape particles are corresponding to MCM-41. This shape is usually form of detecting mesoporous materials with hexagonal pores. The other particles, surrounding MCM-41 seems to be Cu(II) particles.

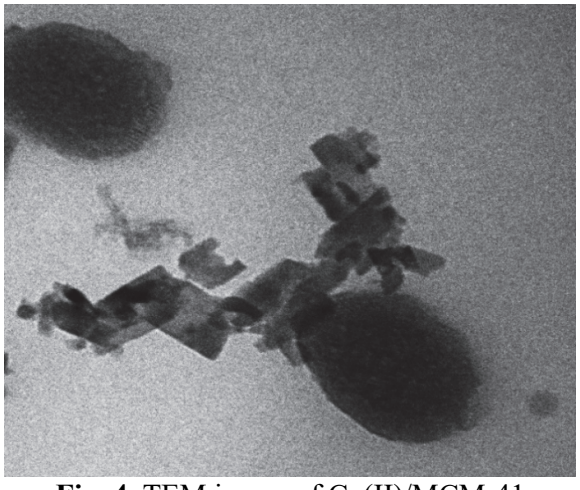

Fig. 4. TEM image of Cu(II)/MCM-41

3.5. BET analysis

After applying the adsorption/desorption of N_2, a type A hysteresis ring formed for MCM-41 **Fig. (5a)**. The observed hysteresis ring for the composite was type B, including mulberry slope in both adsorption and desorption, which illustrated that pores are formed by two parallel sheets. It can be said that usually B-type hysteresis rings is caused be capillaries that have pores which are shaped like ink cans with a very wide body. By considering the **Table 3**, it is obvious that MCM-41 has a virtually large surface area, however, after loading Cu(II) particles on in its surface area decreased by virtually ten times. Besides, after loading its pore volume also declined, which is an evidence that Cu(II) particles are substituted in side MCM-41 pores.

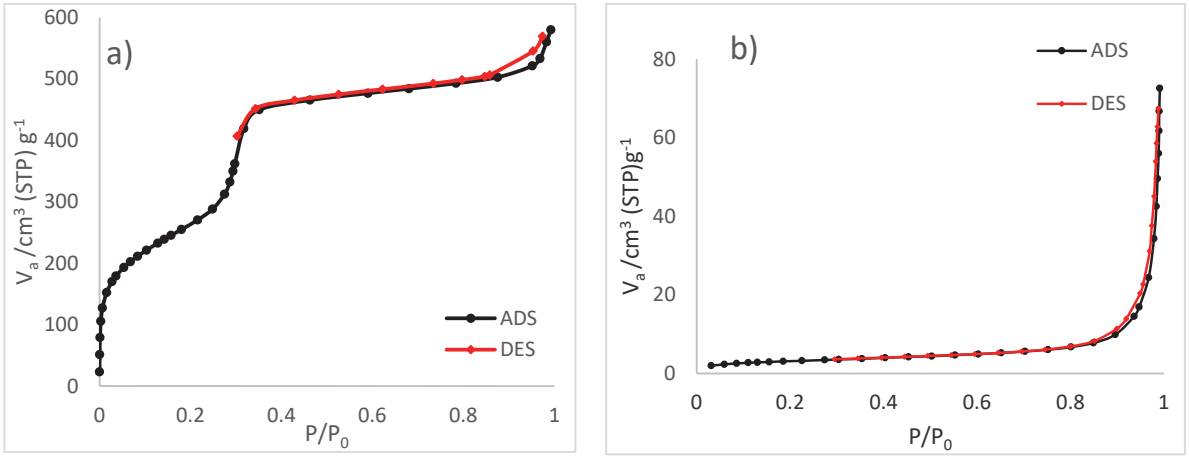

Fig. 5. Adsorption/Desorption isotherm of a) MCM-41 and b) Cu(II)/MCM-41

Table 3. Summary of BET and BJH Plots

	Total pore volume(cm^3/g)	Mean pore diameter (nm)	$a_{s,\,BET}$ (m^2/g)	V_m (cm^3(STP)/g)
MCM-41	0.8901	4.01	904.15	207.73
Cu(II)MCM-41	0.1050	36.71	105.87	2.4801

4. Results Design of Experiment

4.1. Effect of pH

Due to studying the effect of pH, some experiments at various pH levels were performed. By evaluating the obtained data, it was proved that the pH plays the most crucial role in the efficiency of indole removal. The amount of pH determined the surface charge of the composite, which was evaluated by using pH_{pzc} in pH 4, 7 and 10. At the lower amount of pH (4), the catalyst surface charge was negative (-7), that of neutral pH was about 4.4, also, at higher pH level (10), the ratio of sites with positive charge enhanced (8.8). The results of experiments show that the increasing pH value increased the removal efficiency. Although it was found that the efficiency of the catalyst was larger in the indoles lower concentration, the effect of pH was effective to the point that at higher amount of pH, regardless of indole initial concentration, the highest efficiency will obtained.

4.2. Effect of Mass of Catalyst

It was found that by increasing the mass of catalyst as the amounts of available active sites and the contact level increased, the efficiency increased. The highest efficiency obtained at 1g mass of the catalyst (**Fig. 6**).

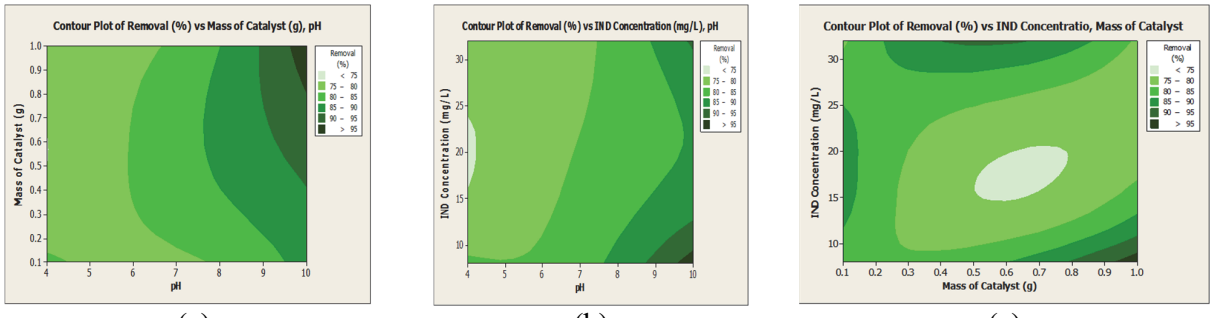

(a) (b) (c)

Fig. 6. Contour plots of Removal efficiency versus a) pH and Mass of catalyst, b) pH and IND concentration and pH, c) Mass of catalyst and IND Concentration.

4.3. Effect of Indole Initial Concentration

As the indole concentration enhanced the efficiency experienced an increase, which shows that the prepared catalyst is a suitable catalyst for removal pollutant even in high concentration of the contaminant (**Fig. 7**).

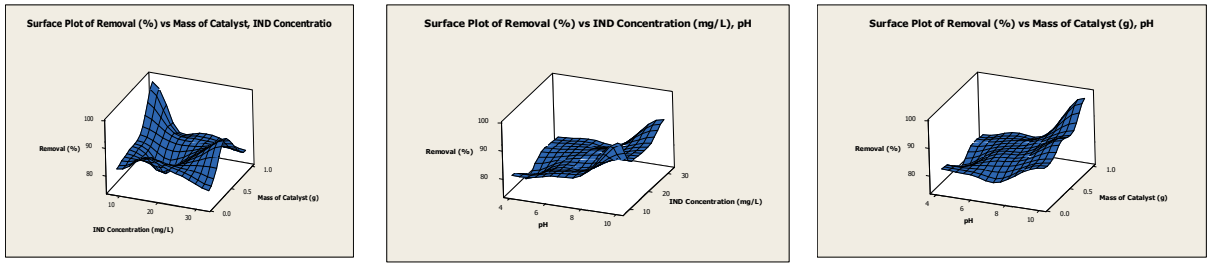

(a) (b) (c)

Fig. 7. 3D plots of removal efficiency versus a) pH and Mass of catalyst, b) pH and IND concentration, c) Mass of catalyst and IND Concentration.

4.4. Optimum condition

By considering the obtain results, the optimum conditions are obtained: pH 10, indole concentration 8 mg/L, and 1.0 mass of catalyst. Factors in term of their influence are pH> IND Concentration>Mass of Catalyst. **Fig. 4** illustrated the mean of S/N ratio graphs. It is also predicted that under optimum condition the removal efficiency will be 98.77% (**Fig. 8**).

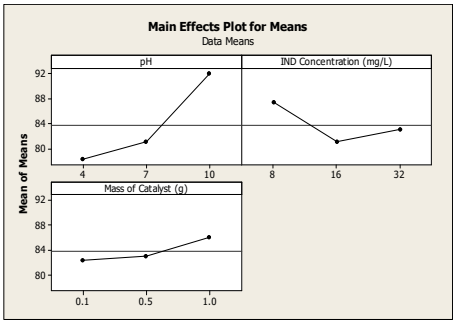

Fig. 8. Mean of means graph for pH, IND concentration, and Mass of catalyst

5. Conclusion

First Cu(II)/MCM-41 was synthesised and characterized by various methods. Second, it was harnessing for indole oxidation in room temperature. After performing the suggested experiments by the software, it was found that the prepared Cu(II)/MCM-41 composite is an efficient and inexpensive, catalyst for indole oxidation, under UV irradiation. By applying the Taguchi method, the oxidation conditions was optimized which was included: pH 10, 8 (mg/L) indole initial concentration and 1 g mass of catalyst. The obtained results illustrated that factor pH was the most important factor. It is also predicted by software that in such optimum operating circumstances highest amount of efficiency (98.77%) will be achieved

References

1 Liu, Y., Wang, L., Huang, Z., Wang, X., Zhao, X., Ren, Y., Ma, J. (**2018**). Oxidation of odor compound indole in aqueous solution with ferrate (VI): Kinetics, pathway, and the variation of assimilable organic carbon. *Chemical Engineering Journal*, *331*, 31-38.

2 Chen, J., De Crisci, A. G., & Xing, T. (**2016**). Review on catalysis related research at CanmetENERGY. *The Canadian Journal of Chemical Engineering*, *94*(1), 7-19.

3 Wu, Y. C., Yang, X. F., & Hao, L. (**2017**). Improved oxygen optical sensing performance from Re (I) complex

doped MCM-41 composite samples by incorporating oxadiazole ring into diamine ligand: synthesis, characterization and sensing response. *Sensors and Actuators B: Chemical*, *244*, 1113-1120.

4 Liew, K. Y., Yee, A. H., & Nordin, M. R. (**1993**). Adsorption of carotene from palm oil by acid-treated rice hull ash. *Journal of the American Oil Chemists' Society*, *70*(5), 539-541.

5 Fard, N. E., Fazaeli, R., Yousefi, M., & Abdolmohammadi, S. (2019). Morphology-Controlled Synthesis of CuO, CuO Rod/MWW Composite for Advanced Oxidation of Indole and Benzothiophene. *ChemistrySelect*, *4*(33), 9529-9539.

6 Yao, Q., Xu, L., Han, Z., & Zhang, Y. (**2015**). Production of indoles via thermo-catalytic conversion and ammonization of bio-derived furfural. *Chemical Engineering Journal*, *280*, 74-81.

7 Linhares, M., Rebelo, S. L., Simões, M. M., Silva, A. M., Neves, M. G. P., Cavaleiro, J. A., & Freire, C. (**2014**). Biomimetic oxidation of indole by Mn (III) porphyrins. *Applied Catalysis A: General*, *470*, 427-433.

8 Liu, Y., Wang, L., Huang, Z., Wang, X., Zhao, X., Ren, Y., Ma, J. (**2018**). Oxidation of odor compound indole in aqueous solution with ferrate (VI): Kinetics, pathway, and the variation of assimilable organic carbon. *Chemical Engineering Journal*, *331*, 31-38.

9 Zhou, X. R., Hong, M. A., FU, X. M., YAO, C. B., & XIAO, J. Q. (**2010**). Catalytic oxidation of carbazole using t-butyl hydroperoxide over molybdenum catalysts. *Journal of Fuel Chemistry and Technology*, *38*(1), 75-79.

10 Chester, A. W., & Derouane, E. G. (**2009**). *Zeolite characterization and catalysis* (Vol. 360). New York, EUA: Springer.

11 Lee, S. Y., & Park, S. J. (**2013**). Determination of the optimal pore size for improved CO2 adsorption in activated carbon fibers. *Journal of colloid and interface science*, *389*(1), 230-235.

12 Perot, G., & Guisnet, M. (**1990**). Advantages and disadvantages of zeolites as catalysts in organic chemistry. *Journal of Molecular Catalysis*, *61*(2), 173-196.

13 Rayati, S., Ruzbahani, S. E., & Nejabat, F. (**2017**). A Comparative Study of Catalytic Activity of Fe, Mn and Cu Porphyrins Immobilized on Mesoporous MCM-41 in Oxidation of Sulfides. *Macroheterocycles*, *10*(1), 62-67.

14 Nikoorazm, M., Ghorbani-Choghamarani, A., & Khanmoradi, M. (**2016**). Synthesis and characterization of Ni (ii)–Vanillin–Schiff base–MCM-41 composite as an efficient and reusable nanocatalyst for multicomponent reactions. *RSC Advances*, *6*(61), 56549-56561.

15 Wei, X. N., Wang, H. L., Li, Z. D., Huang, Z. Q., Qi, H. P., & Jiang, W. F. (**2016**). Fabrication of the novel core-shell MCM-41@ mTiO2 composite microspheres with large specific surface area for enhanced photocatalytic degradation of dinitro butyl phenol (DNBP). *Applied Surface Science*, *372*, 108-115.

16 Kashi, N., Fard, N. E., & Fazaeli, R. (**2017**). Empirical modeling and CCD-based RSM optimization of Cd (II) adsorption from aqueous solution on clinoptilolite and bentonite. *Russian Journal of Applied Chemistry*, *90*(6), 977-992.

17 Tamoradi, T., Ghadermazi, M., & Ghorbani-Choghamarani, A. (**2018**). Highly efficient, green, rapid, and chemoselective oxidation of sulfur-containing compounds in the presence of an MCM-41@ creatinine@ M (M= La and Pr) mesostructured catalyst under neat conditions. *New Journal of Chemistry*, *42*(7), 5479-5488.

18 Taguchi, G. (**1990**). Introduction to Quality Engineering, Tokyo. *Asian Productivity Organization*.4(2), 10-15.

19 Fard, N. E., & Fazaeli, R. (**2018**). Optimization of Operating Parameters in Photocatalytic Activity of Visible Light Active Ag/TiO 2 Nanoparticles. *Russian Journal of Physical Chemistry A*, *92*(13), 2835-2846.

20 Nikoorazm, M., & Ghobadi, M. (**2019**). Cu-SBTU@ MCM-41: As an Efficient and Reusable Nanocatalyst for Selective Oxidation of Sulfides an Oxidative Coupling of Thiols. *Silicon*, *11*(2), 983-993.

21 Brazlauskas, M., & Kitrys, S. (**2008**). Synthesis and properties of CuO/Zeolite sandwich type adsorbent-catalysts. *Chinese Journal of Catalysis*, *29*(1), 25-30.

22 Ghorbani, M., & Nowee, S. M. (**2016**). Kinetic study of Pb (II) and Ni (II) adsorption onto MCM-41 amine-functionalized nano particle. *Advances in environmental technology*, *2*, 101-104.